



Railway ballast degradation

José Pires, LAVOC-EPFL
André-Gilles Dumont, LAVOC-EPFL

Conference paper STRC 2015

STRC

15th Swiss Transport Research Conference
Monte Verità / Ascona, April 15-17, 2015

Railway ballast degradation

José Pires
LAVOC, EPFL
Lausanne

André-Gilles Dumont
LAVOC, EPFL
Lausanne

Phone: + 41 21 6932348
Fax: + 41 21 693 6349
email: jose.pires@epfl.ch

Phone: +41 21 6932389
Fax: + 41 21 693 6349
email: andre-gilles.dumont@epfl.ch

April 2015

Abstract

The ballast layer of the railway profile is composed of cubic grains in fractions of between 22.0-63.0 mm and comprises one of the most important elements of the railways playing a key role in its behaviour with regard to mechanical and hydraulic properties, and track maintenance efficiency.

Due to traffic and maintenance procedures, over time, the ballast material is subjected to degradation via wear and breakage phenomenon. In order to represent this degradation, abrasion and large-scale tests can be performed. This paper presents an overview concerning ballast degradation due to loading and maintenance procedures and results obtained from samples submitted to Los Angeles Abrasion and large-scale tests. An image-based process was also employed to evaluate degradation evolution based on the roundness index.

The objective of this paper is to visualise ballast degradation evolution in terms of granulometric and shape deviations and distinct degradation modes such as the wear and breakage that can occur as a result of the stresses related to traffic and maintenance.

The degradation study showed generally, the granulometric deviation from the highest to the lowest granular fractions, different degradation features specially related to the breakage mode and an adequate representation of the wear degradation evolution via the use of an image-based method. Moreover, analysis in full-scale tests showed a clear difference between the degradation that occurred at different places around the rail-sleeper unit subjected to traffic and tamping action. The phenomenon of ballast degradation due to traffic and maintenance actions is also discussed.

Keywords

Railway ballast – ballast degradation – ballast behaviour

1. Ballast layer

Ballast is the granular upper layer of the superstructure part of the railway track profile and is composed of cubic uniformly-graded grains (22.0-63mm) in a compacted condition and surrounding voids. This layer is placed between the sleepers and platform (or possibly, sub-ballast) with functions related to some of the most important characteristics of the railway track in terms of strength, deformability and drainage.

The functions of the ballast layer are basically to provide a solid foundation for the sleepers, adequate drainage, uniform load distribution allowing flexibility and reconstitution of levelling and furthermore, provide noise and vibration absorption (Selig & Waters, 1994). The layer performs a fundamental role in railway track behaviour resisting to vertical forces by grains direct resistance while lateral and longitudinal forces are equilibrated by the friction generated between ballast particles and the sleepers and between the grains themselves.

The ballast layer capability to perform its function is determined by the physical state of assembly and grain characteristics in terms of size, shape, and strength among other things. Oda and Iwashita (1999) argued that the behaviour of granular materials is determined by particle arrangement and inter-particle characteristics. According to Raymond (1985), the geometrical characteristics of particles are of critical importance for track stability.

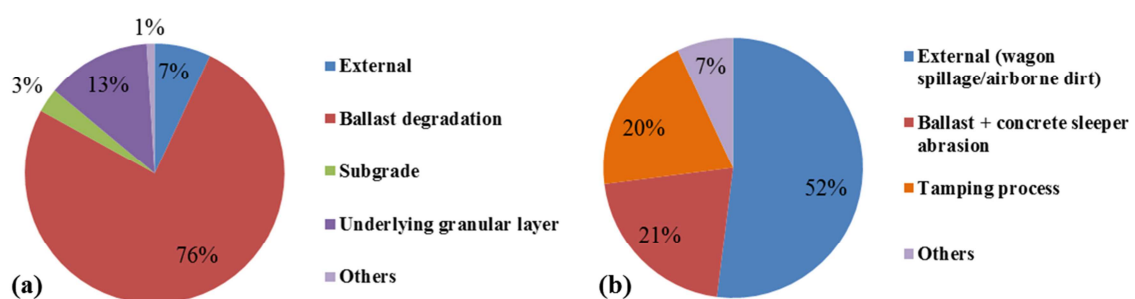
Ballast grains naturally interact with other particles creating contact points. Depending on the stress magnitude due to traffic and/or maintenance procedures at grain contact points, particles may start to degrade with time, which can lead to loss of mechanical performance. Therefore, the study of ballast material subjected to traffic and maintenance conditions is an important task in order to obtain an estimation of degradation evolution.

2. Ballast degradation

As a result of traffic accumulation and maintenance procedures, the ballast layer starts to degrade and this can lead to a loss of performance in terms of mechanical properties and track geometric condition. Ballast layer degradation is caused by phenomena related to wear and grain breakage leading to the filling of granular voids and is known as ballast contamination /fouling.

Ballast layer contamination is caused by different mechanical and environmental phenomena such as grain degradation, fine material pumping, external input (i.e. wagons material), sleeper/grain abrasion, weathering, etc. According to Selig & Waters (1994), data from the UK showed that the main source of contamination was external input (52%) and grain damage including tamping actions (41%). However, US data indicate that the most important source of fouling is grain breakdown (76%) including damage related to traffic, maintenance, weathering and general stresses (Figure 1). In general, the values presented show the significance of the amount of fouling material resulting from ballast grain degradation due to traffic and maintenance actions. Moreover, studies conducted by the Association of American Railroads (AAR) using petrographic analysis indicated that 75-90% of the fouling material accumulated during 300 million gross tonnes (MGT) was from ballast breakdown, and the remainder, from external sources.

Figure 1 Contribution of processes to ballast degradation according to data from USA (a) and UK (b).



Ballast particles degradation can be understood as grain crushing in terms of breakage and abrasion and is a decisive factor in ballast behaviour (Indraratna et al., 1998). According to Lekarp et al. (2000), crushing is a progressive process starting at relatively low stresses and results in gradual changes in granular fabric and packing. According to Terzaghi & Peck (1962), the mechanism of rockfill compression is the result of the crushing of highly stressed contact points and particles rearrangement during load application. A similar mechanism is expected to develop in railway ballast at contact points.

According to Indraratna & Salim (2003), ballast degradation depends on several factors such as the amplitude, frequency and number of load cycles, aggregate density, grain angularity, confining pressures, saturation degree, etc. However, the most significant factor governing ballast breakage is the fracture strength of its constituent particles. Other important factors are the mineralogy and grains shape and size.

Mechanical ballast degradation is related to the dynamic load resulting from traffic accumulation and track condition. As well as traffic, track geometry maintenance actions by means of tamping for example can also provoke considerable grain damage as this method is considered destructive.

Due to traffic and maintenance actions, ballast material can degrade in different modes. According to Raymond & Diyaljee (1979), the ballast grain degradation process can basically occur in three ways: breakage into approximately similarly sized parts, angular projections, and grinding off of small asperities. Figure 2 shows examples of grains degraded by wear (grinding off of small particles) and breakage.

Figure 2 Examples of ballast degradation by wear (a) and breakage (b).



Particle breakage is the dissection of grains into parts occurring generally under high stress levels, while abrasion is a phenomenon whereby very small particles disintegrate from the grain surface, independent of stress level (Indraratna et al., 2011). According to Indraratna et al. (2009), aggregate breakage under rail loading is a complex mechanism initiating at inter-particle contacts, followed by breakage of the weaker particles upon further loading.

Indraratna et al. (2005) identified that most ballast degradation is primarily the consequence of corner breakage that with considerable wear/abrasion can lead to a grain with a relatively more rounded shape. Under traffic conditions, the shock and high pressure induced by the dynamic load distributed through the contact surface in the corners between the grains and the sleeper creates a stress distribution channel. The stress concentration at these corners can provoke its own breakage and tends to grind the portion of the ballast material under the sleepers especially.

Since ballast grains are highly inhomogeneous in nature, the description of breakage mechanisms is no easy task. According to Lu (2008), it relies heavily on visual observation requiring a measure of personal judgment.

As a result of ballast grain degradation, material of different granular fractions is generated including fine material (smaller than a specific diameter, e.g. 14 mm). Generally speaking, an amount of about 30% of fine material is assumed to indicate a fouled granular layer and a

possible end of ballast life (Lichtberger, 2005; Selig & Waters, 1994; Esveld, 1993). According to Paderno (2010), the costs of ballast maintenance represents approximately 30% of the annual track maintenance budget.

Under stress from both traffic and maintenance, the granulometry of ballast material is deviated with consequences to the porous media related to void ratio/porosity decrease. Moreover, degradation also affects grain shape, leading to a tendency towards roundness that is related to the general behaviour of the layer in terms of deformability, strength and permeability. For example, as a result of wear or even breakage, the generation of fine material can provoke the appearance of unexpected negative pore-pressures (e.g. suction) leading to changes in strength and permeability. Related to grain changes in terms of size and shape, degradation can provoke mechanical responses affecting traffic and maintenance performance.

Track maintenance by means of tamping allows a rapid geometry correction but, at the same time, degrades the grains especially during the insertion of vibrating tines. According to Aursudkij (2007), the insertion of the tines breaks large aggregates while grain squeezing causes wear on their surface as occurs during traffic loading (both produce lower and similar degradation). Perales et al. (2011) concluded that tamping provokes grain stresses as it is more like a shock than a phenomenon spread over time, such as wear. Nurmikolu (2005) reported a survey by Chrismer (1988) concerning ballast material subjected to traffic and maintenance during a period of three years that showed significant degradation caused by tamping since the latter changed the granulometry more than traffic did during this period. As a result of frequent tamping actions, the track becomes involved in a vicious circle where degradation from tamping constitutes an important element of dynamic overloads that accelerate geometry deterioration, thus requiring a new geometry correction. The final consequence is that over time, the ballast can lose its fundamental properties and then can no longer assume its functions and has to be replaced.

During degradation, the grain shape variation can indicate certain features regarding the damage processes. According to Mvelase et al. (2012), geometric indexes such as sphericity and roundness can be used to evaluate ballast shape properties. Roundness is defined as the ratio of the sum of the radius of the corners and the radius of the maximum inscribed circle divided by the number of evaluated grains (Wadell, 1932). This can also be calculated via the grain area and perimeter.

In order to simulate ballast grain degradation, abrasion tests such as the Los Angeles (LAA), Mill (MA) and Micro Deval (MDA) can be employed and are an important basis for ballast suitability evaluation (Selig & Boucher, 1990). Moreover, large-scale triaxial tests (Fortunato, 2005; Ionescu, 2004) and traffic/tamping apparatus (Paderno, 2010; Aursudkij, 2004) have been used to evaluate ballast degradation under different traffic and tamping conditions.

Röthlisberger et al. (2006) stated that LAA tests show a correlation with wear induced by railway traffic unlike the conclusion of Aursudkij (2007) that associated the LAA test results to tamping degradation. The author also states that ballast ageing is primarily related to maintenance works as observed by Aursudkij (2007) and the critical environment of ballast ageing is limited to the material volume affected by tamping.

In order to study ballast degradation, analyses were performed to evaluate degradation evolution with data from Paderno (2010) using large-scale apparatus to simulate traffic and tamping conditions, and data from LAA tests carried out using an imaging procedure.

2.1 Degradation rates

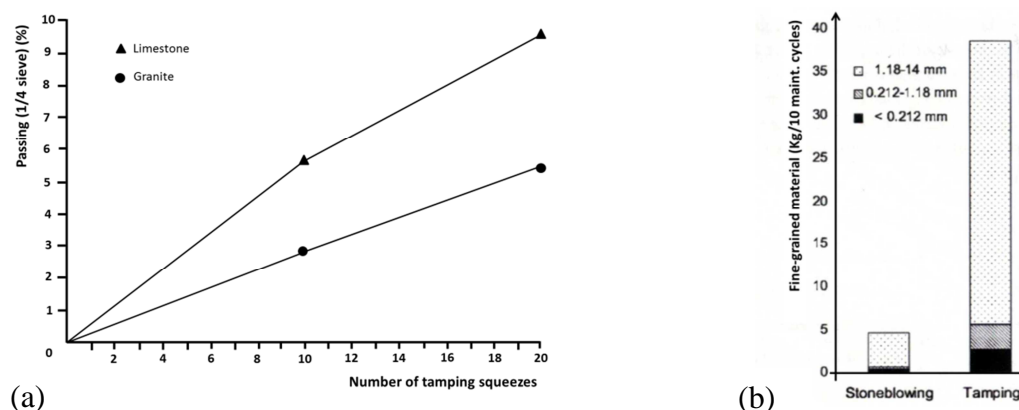
a) Ballast degradation due to tamping process

Since tamping is one of the most common maintenance techniques for restoring track geometry, the planning of ballast maintenance programs is of particular importance. Studies have been carried out to verify the influence of tamping actions on ballast degradation.

A study carried out by AAR (1990) through a series of in-track tests showed the tamping significance on the fine material ($\leq 1/4''$ sieve) generation after 10 and 20 tamping's (Figure 3a). Results showed an almost linear relationship between the number of tamping's and the fine material amount and a production of between 0.45-0.9 Kg of fouling per squeeze. Similar results concerning the linear trend between fouling material generation and number of tamping actions were also found by Rothlisberger (2000) and Aursudkij (2007). According to the latter author, unlike what occurred with ballast material during tines insertion, material from the squeezing region was not influenced by the number of tamping's.

Zarembski & Newman (2008) reported data comparing ballast degradation at both tamping and stone blowing maintenance methods (Figure 3b). The results revealed that a much larger amount of fine material originated from the tamping with a production of approximately 4 Kg per action. These rates are similar to those found on UK railways (Selig & Waters, 1994).

Figure 3 Fine material amount produced by number of tampings for different ballast materials (a) and different maintenance techniques (b).



Perales et al (2011) evaluated the influence of the tamping process in the ballast degradation in a real scale track. The results showed fragmentation of particles greater than 50 mm leading to an increase in the proportion of grains in the granular fraction of 35.5-50.0 mm. With regard to wear degradation, the analysis showed that this seems to become significant when the number of cycles exceeds 20. According to Selig & Waters (1994), data from UK field investigations showed that about 20 consecutive tines insertions resulted in a 15-45% reduction in the 38-51 mm fraction. As far as the fraction smaller than 13 mm was concerned, an increase from about 1% to 5% was observed after tamping's.

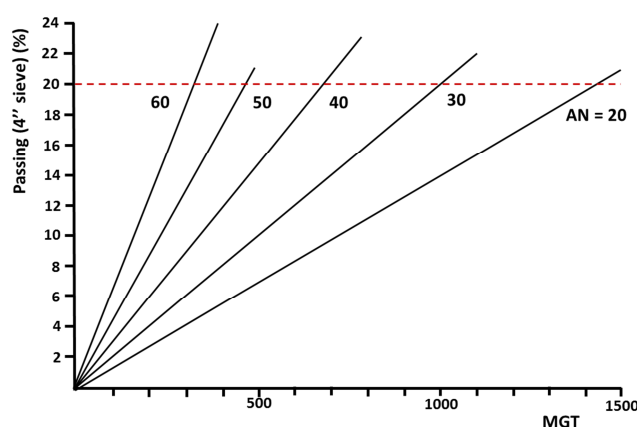
It can be asserted that tamping is a very significant factor in the degradation of ballast and, because of this, unnecessary actions must be avoided. According to the studies, the fouling amount generated seems to be approximately 4 Kg/tamping with material in the tines insertion region being more affected. Moreover, the relationship between the fouling content and tamping actions number seems to be proximately linear.

b) Degradation due to traffic

In order to represent the degradation due to railway traffic, laboratory (cyclic tri-axial, ballast boxes) and large-scale tests can be performed. Indraratna & Salim (2003) applied cyclic loading to railway ballast samples, obtaining a degradation of used ballast of roughly two times that of a new material. However, ballast degradation in cyclic triaxial tests was found to be very low and thus not to correspond to degradation under field conditions by Raymond & Bathurst (1994), among others.

AAR (1989) performed a study of degradation rates related to ballast quality in terms of Abrasion Number (AN=LAA+5MA) and MGT value. The results showed a clear difference in ballast fouling between ballast materials with different abrasion values (Figure 4).

Figure 4 Example of ballast fouling related to quality and MGT value.



According to Selig & Waters (1994), UK data concerning sources of degradation and its rates, show values of approximately 0.2 Kg/sleeper/MGT of degradation resulting from traffic fouling. The same authors also report on an *in situ* ballast durability study conducted by AAR using granulometric analysis over seven years (300 MGT). After this period, fouling (≤ 4.75 mm) was 5-7 % (initially 1-3%), revealing an increase rate of 0.4-0.6% per year. Linear extrapolation of the degradation rate to a condition of complete fouling gave unreasonably long ballast lives, suggesting that degradation rate is not linear over ballast life.

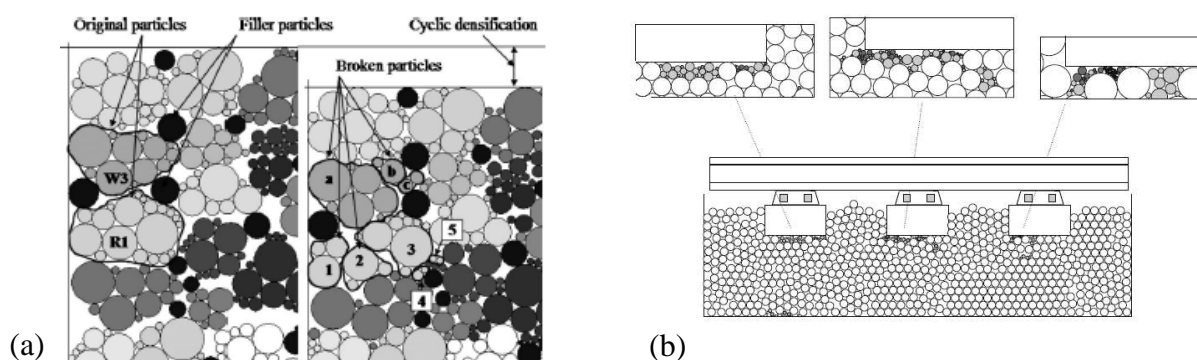
2.2 Numerical modelling of ballast breakage

Normally, discontinuum-based methods treat rock material as an assembled model of particles. Related to fracture, the process can be represented for example by inter-particle bond breakage.

The dominant stream in discontinuum-based modelling is the DEM (Discrete Element Method). DEM is capable of analysing multiple interacting bodies undergoing displacements and rotations. Contact detection and interactions are the most important aspects in the DEM, which is distinguished by its ability to detect (create) new contacts during calculation.

In order to represent particle breakage, several methods have been used as for example, the replacement of particles fulfilling a predefined failure criterion with an equivalent particle group and the consideration of each particle as porous agglomerate built by bonding smaller particles. Figure 5(a) and 5(b) shows examples of ballast grains models according to Indraratna et al. (2010) and Lobo-Guerrero & Vallejo (2005) respectively.

Figure 5 Portion of assembly showing particle breakage (a) and detail of crushable ballast representation (b).



Lobo-Guerrero & Vallejo (2005) treated the particle as porous agglomerate in order to evaluate the crushing evolution in the granular material in a model representative of a railway ballast layer. A breakage criterion based on the coordination number (contacts) and a comparison between the tensile stresses calculated and a threshold value were employed. The particles were treated as agglomerate composed of discs of different sizes and if a particle fulfils the above criterion, it is decomposed, generating smaller ones. In another kind of ballast grain approach, Indraratna et al. (2010) performed a numerical study of the ballast material under cyclic loading using the concept of parallel bonds representing the ballast grains as an agglomerate of particles.

3. Ballast degradation analysis

In order to study ballast degradation evolution at different conditions of efforts, two analyses were performed.

In the first study, laboratory LAA tests were conducted to evaluate the evolution of the ballast material degradation. The results are presented in terms of granulometric deviations and grains shape evolution. Different modes of degradation related to wear and breakage are also evaluated.

Moreover, data from Paderno (2010) were used to evaluate ballast degradation during periods of traffic and maintenance actions. The results were also obtained in terms of granulometric deviations and ballast material place of collection.

3.1 Material

The material studied in both analyses was sandstone ballast with 25-30% of hard minerals, with a particle size of between 22.4 and 63.0 mm and LAA values of between 11 and 15 complying with EN 13450, collected from a quarry that supplies material for the Swiss Federal Railways (CFF/SBB). Figure 6 shows the granulometric curve of the studied material while Table 1 shows some material characteristics comparing them with the values prescribed by Swiss Standard SN 670 110 (Rothlisberger, 2009).

Figure 6 Granulometric curve of studied ballast material.

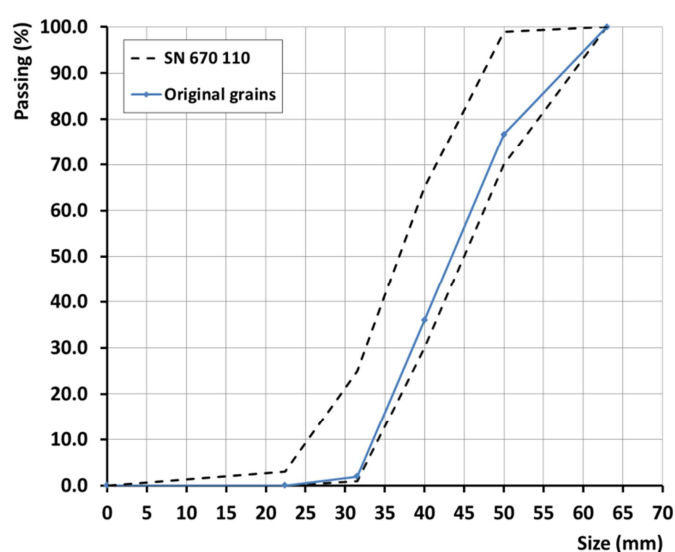


Table 1 Characteristics of ballast material used in studies.

Railway ballast 32/50 – Requirements according to SN 670 110.		
Property	Required value	Value
Fines	$\leq 0.5\%$ (mass)	0.1
Shape index	$\leq 20.0\%$ (mass)	$\approx 11-14$
Long grains	$\leq 4.0\%$ (mass)	0-3
Fragmentation resistance	$\leq 16/24$ (class 1/2)	≈ 14

3.2 Methodology

a) Abrasion tests

In order to simulate material degradation, a ballast sample was subjected to LAA tests. The tests were performed without the steel ball normally used in this kind of abrasion test with the aim of avoiding excessive shocks and promoting abrasion between grains.

The sample was tested at 100, 200, 300 and 400 revolutions. For this purpose, firstly, some of the grains were randomly selected and numbered in order to keep track of them during the tests. At each revolution stage, all the selected grains were weighed and the granulometric curve determined. Furthermore, at each stage, the roundness values of the numbered grains were calculated through 2D images. Then, at the end of each stage, the grains were placed back in the LAA machine for the next testing phase.

In order to obtain the images and visualise the grain degradation during each revolution stage, an apparatus composed of a tripod, bulkhead and fixtures was mounted. From the images taken for each grain at each stage, the roundness value was calculated and the roundness evolution during the revolution stages was evaluated.

As to the quality of the images, they were adjusted in relation to the number of pixels inside the contour of the object, contrasts and lights to avoid any interference related to shadows that could impair the identification of grain degradation characteristics.

Based on the granulometric curve variation over the revolution stages, an evaluation was performed via the granulometric changes at the granular fractions of 0-22.4 mm (fine material), 22.4-31.5mm, 31.5-40.0mm, 40.0-50.0mm and 50.0-63.0mm.

The granulometric curve deviation was also evaluated by the calculation of certain grading coefficients, namely: Coefficient of Uniformity ($C_u = D_{60}/D_{10}$) and Coefficients of Curvature ($C_c = D_{30}^2 / (D_{60} \cdot D_{10})$), where D_{60} , D_{30} and D_{10} are the 60, 30 and 10% passing material found in the granulometric curve. These gradation factors were used to obtain a quantitative measure of the ballast material degradation at each revolution stage.

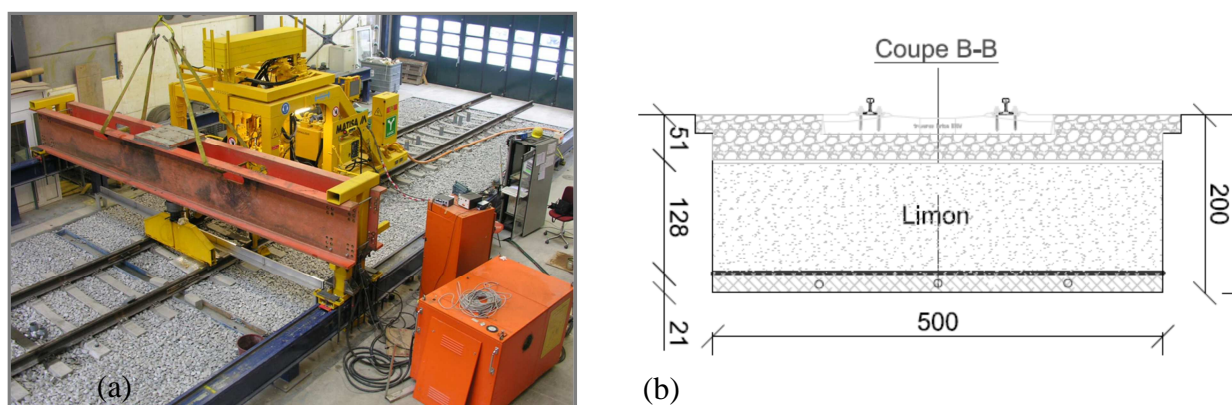
With regard to the degradation mode survey, at each revolution stage, the sample was granulometrically and visually evaluated to identify the degradation modes and main characteristics during each phase.

In order to evaluate degradation evolution based on grain shapes, the initially selected grains were submitted to a roundness evaluation. The grains were photographed and then, after each LAA test stage, pictures were taken for degradation evaluation by means of the roundness index. The roundness value (R) was used to support the ballast degradation evaluation with the aim of measuring the sharpness of the edges and corners of individual grains and was calculated from the ballast grain pictures using the perimeter (P) and area (A) values ($R = 4\pi A/P^2$) obtained from images.

b) Full-scale test

In the second study, data from Paderno (2010) with the same material were used for ballast degradation evaluation. The data were obtained from a large scale apparatus constructed *ad hoc* to simulate traffic and tamping procedures using a static-dynamic cylinder and a real-scale tamper machine respectively. Figures 7(a) and 7(b) shows the test pit used with the beam for load application and the infrastructure profile installed.

Figure 7 General view of test pit test with the beam for load application (a) and infrastructure profile (b).



For the analysis carried out, two scenarios were evaluated:

- Scenario a – Sequence of efforts composed of three tamping actions (depth of 20 mm), followed by an application of 7'000'000 cycles (load of 22.5 ton/axle) and three more deeper tampings (depth of 60 mm) in a soft foundation ($Ev1 \approx 90 \text{ MN/m}^2$, $Ev2 \approx 40 \text{ MN/m}^2$).
- Scenario b – four tamping actions (depth of 20mm) in the same foundation condition.

The tamping actions were performed with a vibration frequency of 42 Hz, an amplitude of 8mm and a lift height of 20mm.

After the scenarios had been simulated, ballast samples were collected around and just below the sleeper to evaluate different quantitative degradation trends by the determination of

granulometric curves. Based on the granulometric variation, an evaluation was performed via the granulometric changes at different granular fractions at the intervals of 0-22.4mm (fine material), 22.4-31.5mm, 31.5-40.0mm, 40.0-50.0mm and 50.0-63.0mm. The granulometric curves deviations were also evaluated using the calculated value of the Coefficient of Curvature (Cc) and Coefficient of Uniformity (Cu).

4. Results

4.1 Abrasive tests

As described, the granulometric curves over the revolution stages were obtained from the LAA tests performed. Figure 8 (a) and (b) shows respectively these curves with the values of Cc and Cu and the granulometric distribution variation at the granular fractions studied.

Figure 8 Granulometric curves and grading factors (a) and granular fractions distribution (b) of tested ballast material.

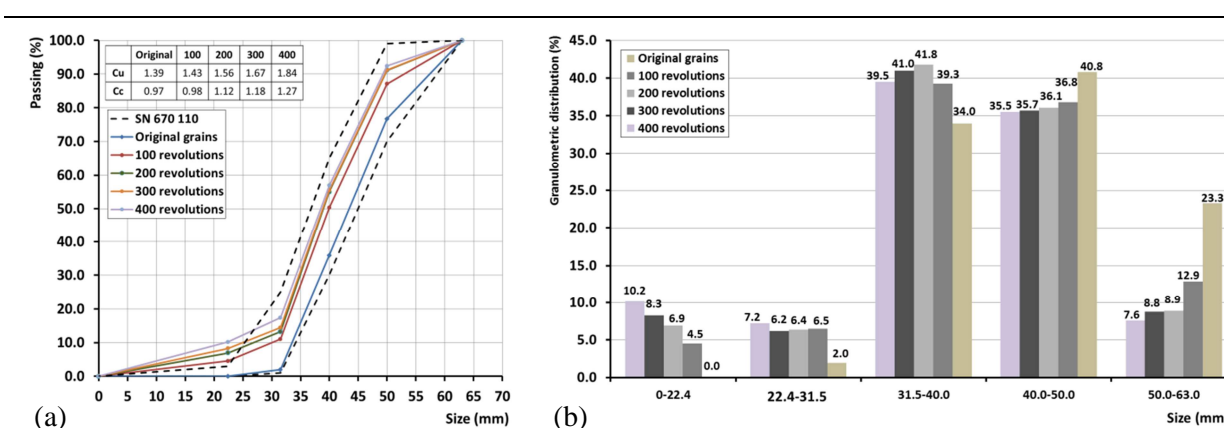


Figure 8 shows that after 100 cycles all the granular fractions were affected by the degradation and the fraction between 0-22.4 already failed to comply with Swiss Standard (SN 670 110) since that the maximum allowed for this fraction is 3% but just after 100 cycles, the value was approximately 4.5%. In the subsequent revolutions, the observed granulometry deviation was lower with a larger increasing and decreasing trend for the 0-22.4 and 50.0-63.0 mm fractions respectively.

In the material amount generated in the fraction 0-22.4 mm there was a clear increase as revolutions increased. The same trend was noticed in the fraction 22.4-31.5 mm with a large increase in ballast quantity just after 100 revolutions and a subsequent low variation. In the fraction 31.5-40.0 mm the results were not conclusive since there was an increase of the ballast particle amount until 200 revolutions with a small subsequent decrease. The granular fractions of 40.0-50.0 and 50.0-63.0 mm showed a similar decreasing trend, far more accentuated in the latter one especially after the first 100 revolutions. Figure 8 (a) also shows an increasing trend of the gradation coefficients Cu and Cc revealing a loss of grade uniformity. This tendency was similar to that obtained for ballast material by Boler et al. (2012) also using the LAA tests.

During the LAA tests performed, different degradation modes in the analysed particles were noted. From the material granulometry, image and visual grain observation, weight and dimension measures, the following types of degradation can be specified:

- Wear degradation – In roughly 64% of particles, a degradation trend was observed with a higher loss of mass in the first 100 revolutions and a subsequent low decrease in mass loss accompanied by an approximately constant increase in roundness index.
- Breakage with wear degradation – In roughly 36% of the material, a degradation trend in terms of breakage accompanied by wear was observed with the following different features:
 - Partial grain breakage – breakage of a small part of the grain (basically, corners) in the first number of revolutions (100, 200) with no creation of an approximately similarly sized second grain and subsequent wear degradation trend. The degradation was characterised by an initial high loss of mass with a subsequent low mass loss related to wear and gradual roundness increase.
 - Full grain breakage – grain breakage with the creation of an approximately similarly size grain in the first number of revolutions. Subsequently, the new grains with their distinct roundness values followed the wear degradation trend characterised by a gradual roundness increase.

The conclusions relating to the breakage modes obtained are in accordance with those mentioned by Raymond & Diyaljee (1979) also for ballast material that stated that the degradation process of ballast particles occurs through particle breakage, angular projection breakage and the grinding off of small asperities.

a) Wear degradation

In the tests performed, wear degradation was characterised by a progressive and more or less linear increase of the roundness value calculated. Figure 9 shows an example of a grain wear degradation evolution over the revolution stages, while Figure 10 shows the calculated roundness value increase through the stages for some of the ballast grains tested.

Figure 9 Evolution of wear degradation in ballast grain over tested revolutions.



Figure 10 Roundness increase for some grains tested through the revolution stages.

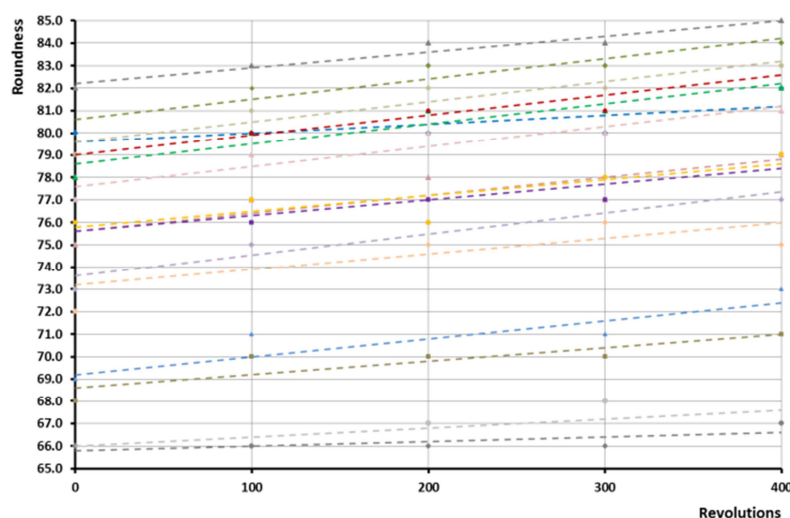


Figure 9 shows a sequence related to the wear degradation evolution with no breakage and a rounding trend on its surface, while Figure 10 shows a smooth and approximately linear roundness increase along the revolutions. Generally, initial grain roundness varied from 57 to 83 with most of the grains having a value of between 70 and 80 and had an increase that varied by up to 5%.

The general behaviour of wear degradation in terms of roundness values calculated along the revolutions revealed an approximately linear trend with correlation values (R^2) varying from 0.5 to 1.0 with most of the grains obtaining values higher than 0.75 and an average of 0.8. Equation 1 shows the linear correlation between the roundness values and the revolution number.

$$R_1 = A \cdot RN + R_0 \quad (1)$$

where:

$R_{1,0}$ = final and initial roundness [-];

RN = revolution number [-];

A = angular coefficient [-].

N.B.: The value of the angular coefficient varied between 10^{-2} and 10^{-3} .

With the aim of gaining a better understanding of the evolution of ballast degradation, a brief statistical analysis via the probability distribution of data related to roundness values in the wear degradation mode was performed. For this, different distribution functions were tested (e.g. Weibull, Normal, Log-normal, Student's) and both Chi-Squared and Kolmogorov-Smirnov criteria were employed for the determination of the distribution function that best

fitted the data evaluated. The results showed that the Weibull distribution function fitted best for the roundness values calculated at all the stages tested (original to 400 revolutions). The Weibull distribution has been found to fit fairly well in several studies conducted focussing on the particle strength analysis (McDowell et al., 1996; Aursudkij, 2007). More details concerning the methods used exceed the scope of this paper but can be found in Weibull (1951).

Figure 11 shows examples of histograms and Weibull curves for the roundness values found for grains tested before (original grains) and after 200 revolutions.

Figure 11 Histograms and Weibull distribution curves for roundness values obtained for original grains (a) and after 200 revolutions (b).

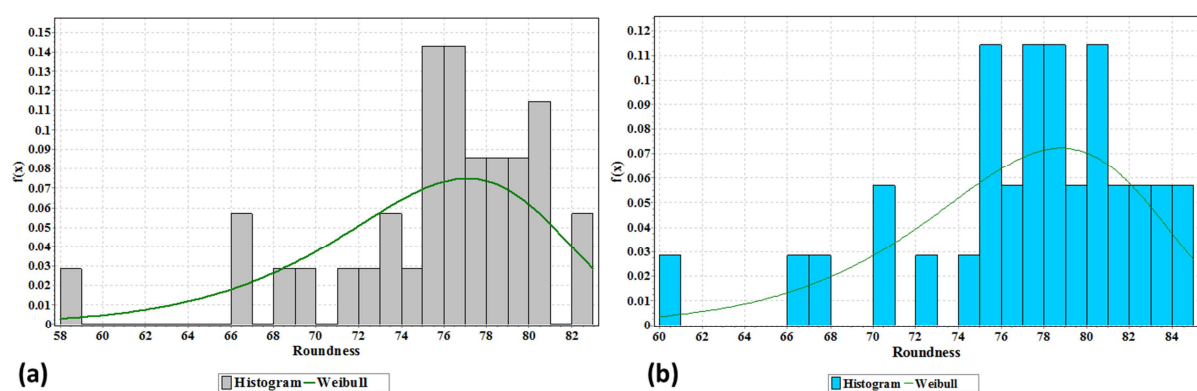


Table 2 shows the general Weibull factors and average, STD and skewness (asymmetry measure of a certain frequency distribution) values over the revolution stages.

Table 2 Weibull and statistic factors over revolution stages.

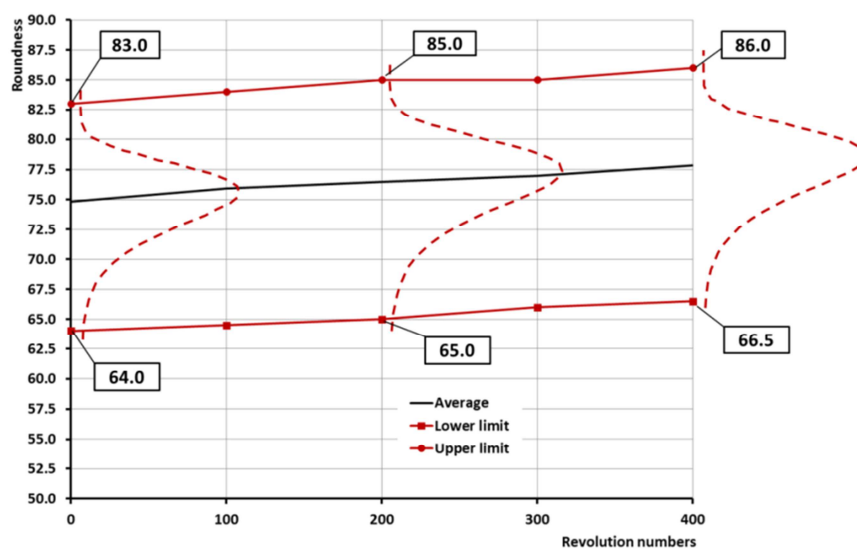
	Original	100	200	300	400
α	15.72	15.62	15.51	15.98	15.81
β	77.41	78.52	79.14	79.56	80.49
average	74.86	75.92	76.50	76.97	77.85
STD	5.85	5.97	6.06	5.92	6.05
skewness	-0.8018	-0.7999	-0.7978	-0.8068	-0.8036

The values in this table reveal very little variation of the Weibull factors, denoting that the data distribution trend remains fairly stable during degradation in the wear mode. Over the

revolution stages, the average value increased almost linearly, and in relation to the skewness values, denoted practically the same asymmetry level where the left tail is longer and the mass of the distribution is concentrated on the right side of the curve, emphasizing that most of the values are closer to the Weibull average.

Figure 12 shows the variation of the average roundness and the confidence interval (90% of confidence) determined with the probability density function (pdf) according to the Weibull function considering the original grains and those after 200 and 400 revolutions.

Figure 12 Confidence levels and average evolution within pdf through stages.



The results showed, in general, an approximately linear behaviour in terms of “rounding trend” in the case of wear degradation when there is no breakage mode involved in the degradation process.

b) Breakage with wear degradation

In about 36% of the tested particles, a degradation trend comprising breakage was observed. The breakage phenomenon was accompanied by the wear degradation trend and occurred with distinct characteristics. Part of the grains suffered a breakage of a small part, especially at the grain corners in the first number of revolutions (100, 200) with subsequent wear degradation trend and no creation of an approximately similarly sized second grain. Figure 13 shows an example of a grain in a partial breakage mode over the stages while Figure 14 shows the calculated roundness values variation over the stages for this degradation mode.

The tests performed showed a breakage process mainly occurring in the first number of revolutions and, subsequently, a wear degradation process takes place with a low mass loss and roundness value increase. In some grains, after breakage, degradation was characterised

by an initial high loss of mass with a subsequent low mass loss mass related to wear during subsequent revolutions.

Figure 13 Evolution of small breakage after initial stages.

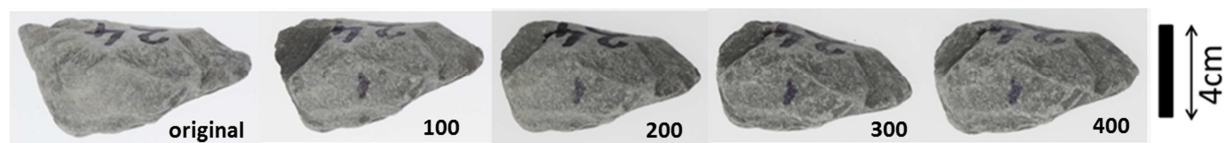
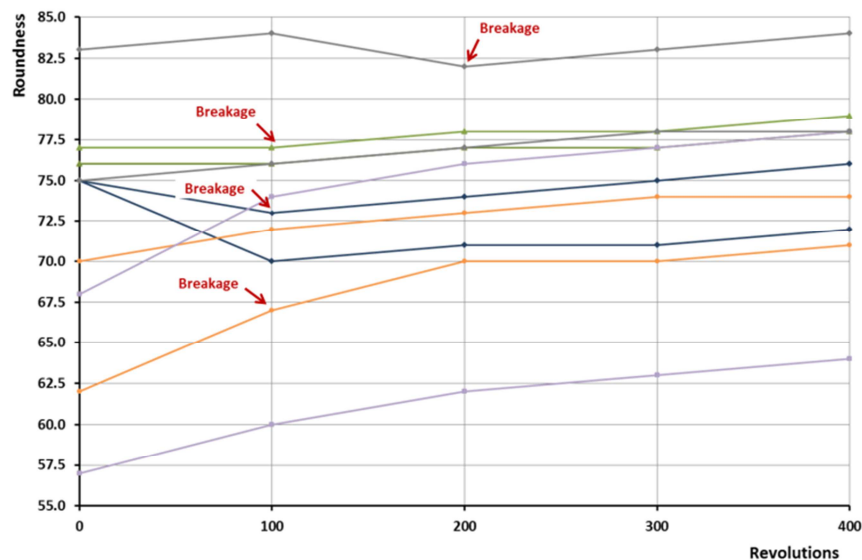


Figure 14 Roundness evolution in case of partial grain breakage with subsequent abrasion degradation trend.



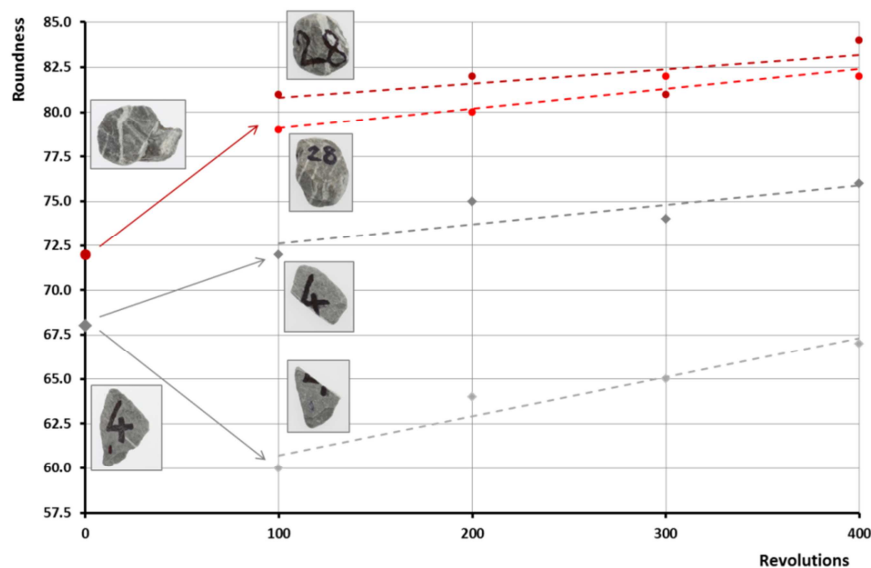
It can also be seen that for some grains that suffered partial breakage, there was just a slight deviation in the roundness value while for others, breakage produced an important change in the roundness as this breakage can impose relevant modifications in grain shape that in some cases resulted in different roundness magnitudes.

Still related to the breakage phenomenon, some grains suffered a full breakage characterised by a clear grain division into approximately two similarly sized parts in the first stages. Subsequently, the two new grains followed the wear degradation trend with a new roundness value and a very low mass loss and roundness value increase. Figure 15 shows the roundness variation in two grains related to this degradation mode over the revolution stages.

From Figure 15, it can be seen that in this breakage degradation mode, an initial breakage produced new particles with independent roundness values. The newly divided grains then underwent their own degradation related to the wear degradation mode.

As shown in the wear degradation mode, in breakage degradation case there was also a good linear correlation (average of 0.76) between the increase of the roundness value and the revolution number.

Figure 15 Roundness evolutions with complete grain breakage with subsequent abrasion trend.



As shown in the case of ballast degradation composed only of wear degradation, the statistical analysis showed that the Weibull distribution function fitted well with the data related to the wear degradation found in the modes comprising breakage. From this, it can be assumed that the wear degradation trend was similar in all degradation modes during the tests.

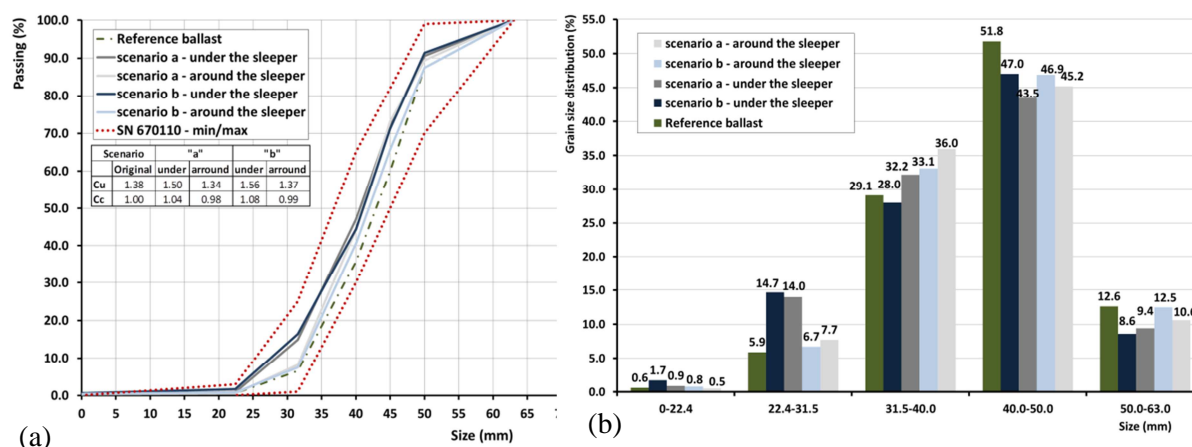
With regard to the degradation modes observed in this study, the wear phenomenon was exhibited by all types and the observed modes are in accordance with those prescribed by Raymond & Diyaljee (1979) in terms of the basic degradation processes such as the wear and breakage phenomenon. However, during the studies it was possible to verify and evaluate some different features such as partial (small) and full breakage and the wear mode within the breakage process.

About the method used to evaluate the degradation, it was possible to ascertain that, especially in cases of wear degradation, it provided an accurate view of the ballast degradation as the image was able to capture the grain rounding trend and calculate the roundness index that generally increased with the number of revolutions.

4.2 Full-scale tests

From the full-scale tests performed to simulate traffic and maintenance conditions, ballast material samples were collected at different places after simulations related to the scenarios *a* and *b* presented above. Figure 16 (a) and (b) shows respectively the granulometric curves and distribution variations (Paderno, 2010).

Figure 16 Granulometric curve (a) and distribution (b) of ballast grains for different scenarios and at different collection points.



From Figure 16, it can be seen that the characteristics of each scenario did not significantly influence degradation considering the same collection place and it therefore seemed to have a secondary influence. However, comparing the collection places, the data showed a clear difference especially regarding the higher percentage of grains in the fraction of 22.4-31.5 mm collected under the sleeper.

With regard to the samples collected under the sleepers, compared to the original distribution, in scenario *a* (traffic and tamping), an increasing trend was observed in the intervals of 0-22.4mm, 22.4-31.5mm and 31.5-40.0mm while in the grains in the fraction of 40.0-50.0mm and 50.0-63.0 mm there was a decreasing trend, unlike what occurred in scenario *b* (tamping only) where there was one single difference related to the decrease in the percentage of grains in the fraction of 31.5-40.0 mm. In the samples collected around the sleeper, both scenarios revealed the same trend with an increase of the percentage of grains of the sizes of 0-22.4, 22.4-31.5, 31.5-40.0 mm and a decrease in the sizes of 40.0-50.0 and 50.0-63.0 mm. Even with the same trend, in scenario *a*, the variations were greater due to the imposed traffic load and the higher number of tamping procedures.

The grading factors (Cc and Cu) were especially affected in the case of samples collected under sleeper where there was a clear loss of uniformity unlike what occurred in samples around the sleepers where the values remained basically constant.

It can be seen that the ballast material collected around the sleepers degraded mainly from the fractions 63.0-50.0 and 40.0-50.0 mm to those of 22.4-31.5 and 31.5-40.0 mm with a higher tendency for the fraction 31.5-40.0 mm, while the ballast material collected under the sleepers revealed the same trend with a difference related to the amount of material in the fraction of

22.4-31.5 mm that was significantly higher compared to the former case. Figures 17 and 18 show the grain size variation in both scenarios with the material collected under the sleeper.

Figure 17 Grain size variation and distribution in samples collected under sleepers in scenario a.

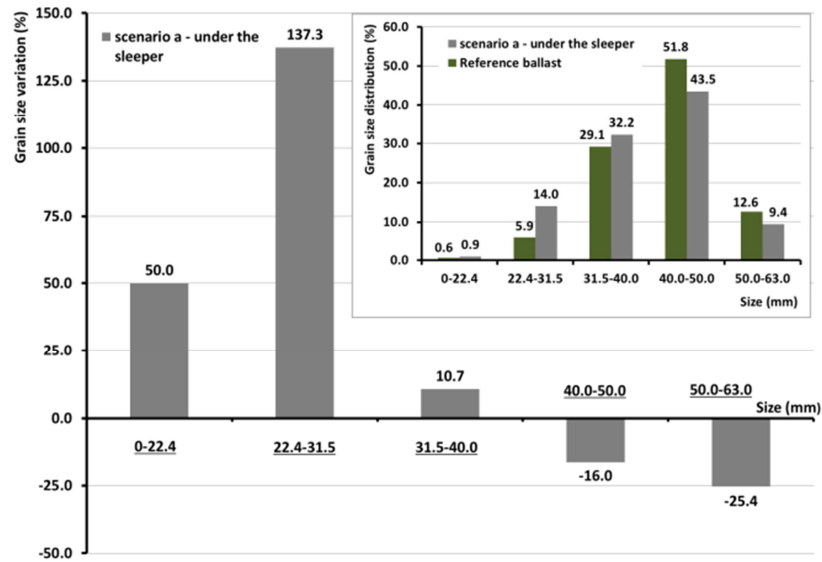
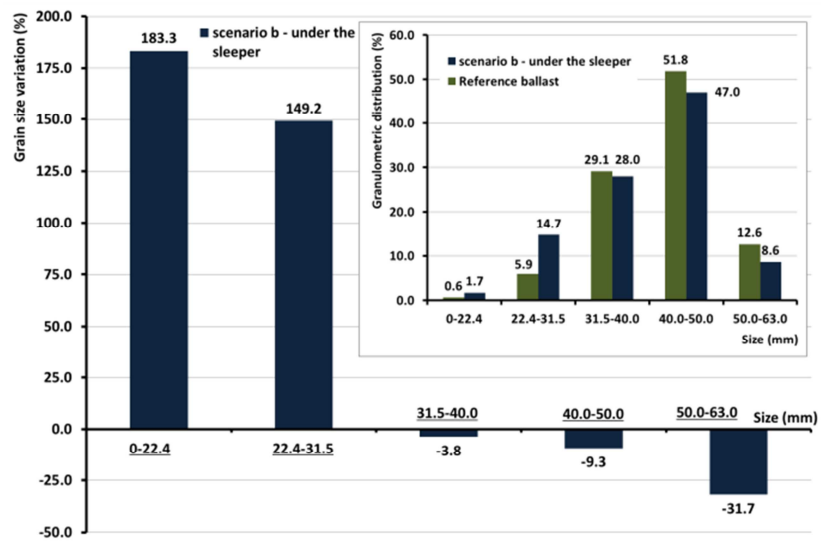


Figure 18 Grain size variation and distribution in samples collected under sleepers in scenario b.



From the figures, in both scenarios, it can be seen that the biggest granulometric increase was related to the granular fractions between 0-22.4 and 22.4-31.5mm, although these fractions are those containing the lowest amount of material (0.6 and 5.9% respectively). Even with a high increase (50 and 183% for scenarios *a* and *b*, respectively), the global amount of material in the fraction of 0-22.4 mm remains low but important due to the fact that basically this fraction is the one related to the fouling material that can lead to a loss of the general mechanical properties of the ballast layer.

In the grain size between 31.5 and 40.0mm, the results showed the opposite variation. In scenario *a*, there was an increase of the quantity of this fraction of 10.7% while in scenario *b*, there was a decrease of 3.8%. The material in the grain fraction between 40.0 and 50.0mm is the particle fraction most present in the global ballast granulometry and its variation revealed a decreasing trend of about 16.0 and 9.3% respectively for scenarios *a* and *b*. The same trend was observed for the fraction between 50.0-63.0mm with a variation of 25.4 and 31.7% for the aforementioned scenarios.

From the large-scale tests, it could be seen that degradation occurred, generating a new amount of ballast material in the fractions between 0 and 31.5 mm from the fractions of 40.0-63.0mm. In the fraction of 31.5-40.0 mm the results were not conclusive as observed in the LAA tests. This gives an indication concerning a possible threshold granular limit around this fraction.

With regard to the degradation of the ballast granular fractions, in both studies a general increasing trend was observed in the ballast sizes of 0.0-22.4 and 22.4-31.5 mm and a decrease in the fractions of 40.0-50.0 and 50.0-63.0 mm.

5. Conclusions

Generally speaking, regarding the granular fractions obtained in both degradation studies, it can be said that degradation basically occurred with the same trends.

The degradation occurred from the fractions of 40.0-50.0 mm and 50.0-63.0 mm to those of 0-22.4 mm (fouling material) and 22.4-31.5 mm. The results related to the fraction of 31.5-40.0 mm were inconclusive, presenting contrary trends. This can indicate a possible threshold granular limit around this fraction value.

With regard to the LAA tests, most of the degradation occurred just after 100 revolutions, and throughout the different stages, different modes of ballast degradation related to wear and breakage were detected.

The wear degradation phenomenon seems to be present in all degradation modes while breakage can occur in a partial or a complete (origin of a size-similar grain) way.

Wear degradation was found to exhibit an approximately linear increase based on roundness value as the revolutions increased while breakage was characterised by the rupture of a grain corner or a larger part resulting in some cases, in new roundness values for the grains involved which, after rupture, tended to follow the wear degradation trend.

The Weibull distribution fitted well with the data of grain roundness due to wear degradation at all stages tested.

The method employed, consisting of the LAA tests with the imaging procedure, allowed the assessment of the ballast degradation, especially in cases of wear degradation.

In the large-scale tests, the scenario did not significantly influence the degradation considering the same collection place and it therefore seemed to have a secondary influence on the degradation unlike the collection place that revealed a remarkable difference in the amount of material originated in the granular fraction of 22.4-31.5 mm collected under the sleeper.

6. References

- AAR (1990) Track Surfacing with Conventional Tamping and Stone Injection, Report N° R-719, Association of American Railroads, USA, 32 pages.
- AAR (1989) Ballast Renewal Model User's Manual, Report N° R-701, Association of American Railroads, USA.
- Aursudkij, B. (2007). A Laboratory Study of Railway Ballast Behavior under Traffic Loading and Tamping Maintenance, *Ph.D. Thesis*, University of Nottingham, UK, 234 pages.
- Boler, H., M. Wnek and E. Tutumluer (2012) Establishing Linkages between Ballast Degradation and Imaging Based Aggregate Particle Shape, Texture and Angularity Indexes, *Advances in Transportation Geotechnics II*, pp. 186-191.
- Esveld, C. (1993) Uniform Ballast Quality Assessment Criteria, Rail Engineering International Edition, N° 2, pp. 11-13.
- Fortunato, E.M.C. (2005) Renovação de Plataformas Ferroviárias – Estudos Relativos à Capacidade de Carga, *PhD Thesis*, University of Porto, 628 pages.
- Indraratna, B & W. Salim (2003) Deformation and Degradation Mechanics of Recycled Ballast Stabilised with Geosynthetics, *Soils and Foundations*, Vol. 43, N°4, pp.35-46.
- Indraratna, B., J. Lackenby and D. Christie (2005) Effect of Confining Pressure on the Degradation of Ballast under Cyclic Loading, *Géotechnique* 55, No. 4, pp. 325-328.
- Indraratna, B., S. Nimbalkar and D. Christie (2009) The Performance of Rail Track Incorporating the Effects of Ballast Breakage, Confining Pressure and Geosynthetic Reinforcement, *Bearing Capacity of Roads, Railways and Airfields*, Taylor & Francis.
- Indraratna, B. and P.K. Thakur, J.S. Vinod (2010) Experimental and Numerical Study of Railway Ballast Behaviour under Cyclic Loading, *International Journal of Geomechanics*, N° 10, pp. 136-144.
- Indraratna, B., W. Salim and C. Rujikiatkamjorn (2011) Advanced Rail Geotechnology – Ballasted track”, CRC press, 414 pages.
- Ionescu, D. (2004) Evaluation of the Engineering Behaviour of Railway Ballast, *PhD Thesis*, University of Wollongong, Australia, 483 pages.
- Lekarp, F., U. Isacsson and A. Dawson (2000) State of the art. I: Resilient Response of Unbound Aggregates, *Journal of Transportation Engineering*, Vol. 126, N° 1, pp 66-75.
- Lichtberger, B. (2005) Track Compendium – Formation, Permanent Way, Maintenance, Economics, Eurail Press, 635 pages.
- Lobo-Guerrero, S. and L. Vallejo (2006) Discrete Element Modelling of Railway Ballast, *Granular Matter* N° 8 (3), pp. 195-204.
- Lu, M. (2008) Discrete Element Modeling of Railway Ballast, *PhD Thesis*, University of Southampton, UK, 245 p.

- McDowell, G.R., M.D. Bolton and D. Robertson (1996) The fractal crushing of granular materials, *Journal of the Mechanics and Physics of Solids*, Vol.44, N°12, pp. 2079-2101.
- Mvelase, G.M., J.K. Boateng and P.J. Grabe (2012) Application of Laser Based Technology to Quantify Shape Properties of Railway Ballast, 31st Southern African Transport Conference, pp. 243-254.
- Nurmikolu, A. (2005) Degradation and frost susceptibility of crushed rock aggregates used in the structural layers of railway track, *PhD Thesis*, Tampere University of Technology, 325 pages.
- Oda, M. and K. Iwashita (1999) *Mechanics of Granular Materials: An Introduction*, A.A. Balkema.
- Paderno, C. (2010) Ballast behavior under action of tamping and railway traffic. *PhD Thesis*, EPFL, Switzerland, 186 p.
- Perales, R., G. Saussine, N. Milesi and Y. Descantes (2011) On the damaging effects of the ballast tamping operation, 9th *World Congress on Railway Research*, 10 pages.
- Raymond, G. P. and V.A. Diyaljee (1979) Railroad Ballast Load Ranking Classification, *Journal of the Geotechnical Engineering*, ASCE 105, N°10, pp. 1133-1153.
- Raymond, G.P. (1985) Research on Railroad Ballast Specification and Evaluation, *Transportation Research Board*, pp. 1-6.
- Raymond, G.P. and R. J. Bathurst (1994) Performance of Large-Scale Model Single Tie-Ballast Systems, *Transportation Research Record*, 1131, pp. 7-14.
- Röthlisberger, F. (2000) Stopfversuch Ostermundigen – Teil II, SBB/CFF Report, 59 pages.
- Röthlisberger, F., J. Cuénoud, L. Chastan, J. Däppen and E. Kuerzen (2006) Compressive Strength of Aggregates on the Stack, VSS 1993/012, 59 pages.
- Röthlisberger, F. (2009) Qualification du Ballast selon R RTE 21110, *Eng.Report*, 15 pages.
- Selig, E.T. and D.L. Boucher (1990) Abrasion Tests for Railroad Ballasts, *Geotechnical Testing Journal*, Vol. 13, Issue 4, pp. 301-311.
- Selig, E. T. and J.M. Waters (1994) *Track Geotechnology and Substructure Management*. Thomas Telford Services Ltd,
- SN 670-110/EN 13450 (2002) Granulats pour Ballasts de Voies Ferrées.
- Terzagui, K & R.B. Peck (1962) *Soil mechanics*, Ao livro tecnico S.A., 659 pages.
- Zaremski, A.M. and G.R. Newman, (2008) Comparative Technical and Economic Analysis of Stoneblowing vs. Tamping, *AREMA - Annual Conference and Exposition*, 32 pages.
- Wadel, A.D. (1932) Volume, shape and roundness of quartz particles, *The Journal of Geology*, Vol. 40, No 5, pp.443-451
- Weibull, W. (1951) A statistical distribution function of wide applicability, *ASME Journal of Applied Mechanics*, N° 18, pp. 293-297